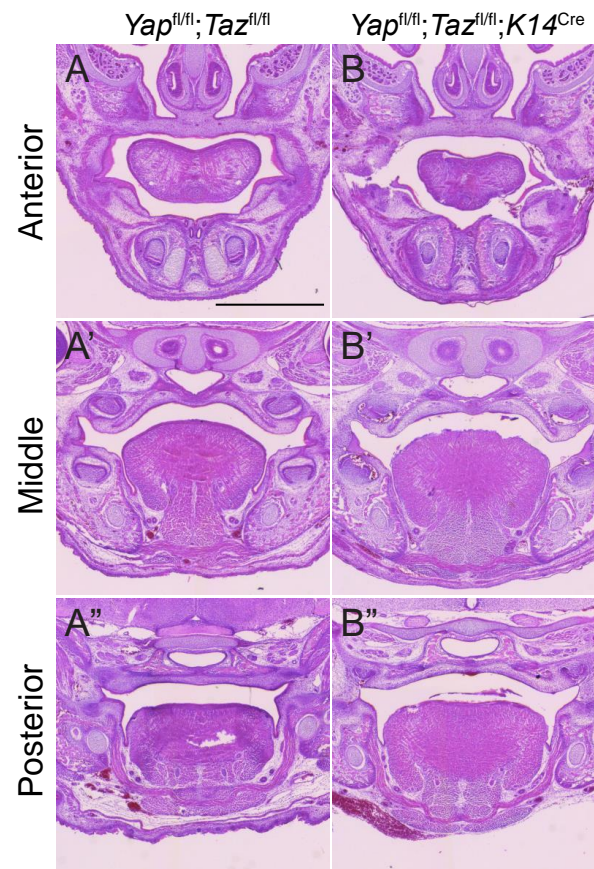


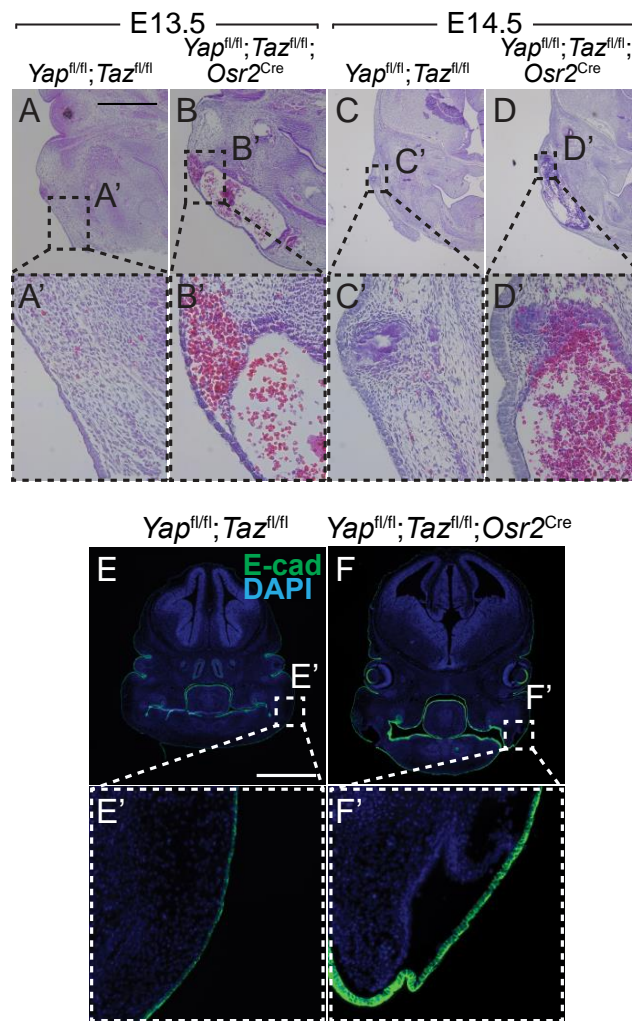
Supplemental Figure 1. YAP/TAZ are expressed throughout the palatal shelf epithelium and mesenchyme. (A-C'') Immunofluorescence with antibody against YAP showing that YAP was highly expressed in the dental epithelium (white asterisks), palatal shelf epithelium (white arrowheads), and palatal shelf mesenchyme (green arrowheads) in the anterior (A,B,C), middle (A',B',C'), and posterior (A'',B'',C'') palatal shelves at E12.5 (A-A''), E13.5 (B-B''), and E14.5 (C-C''). Of note, significant YAP expression was found in the ossification region in the posterior palatal shelf at E14.5 (white dashed circle). (D-F'') Similarly, TAZ was expressed in the epithelium and mesenchyme of the palatal shelves from anterior to posterior, throughout development. Scale bar=200 μ m.

Supplemental Figure 2.

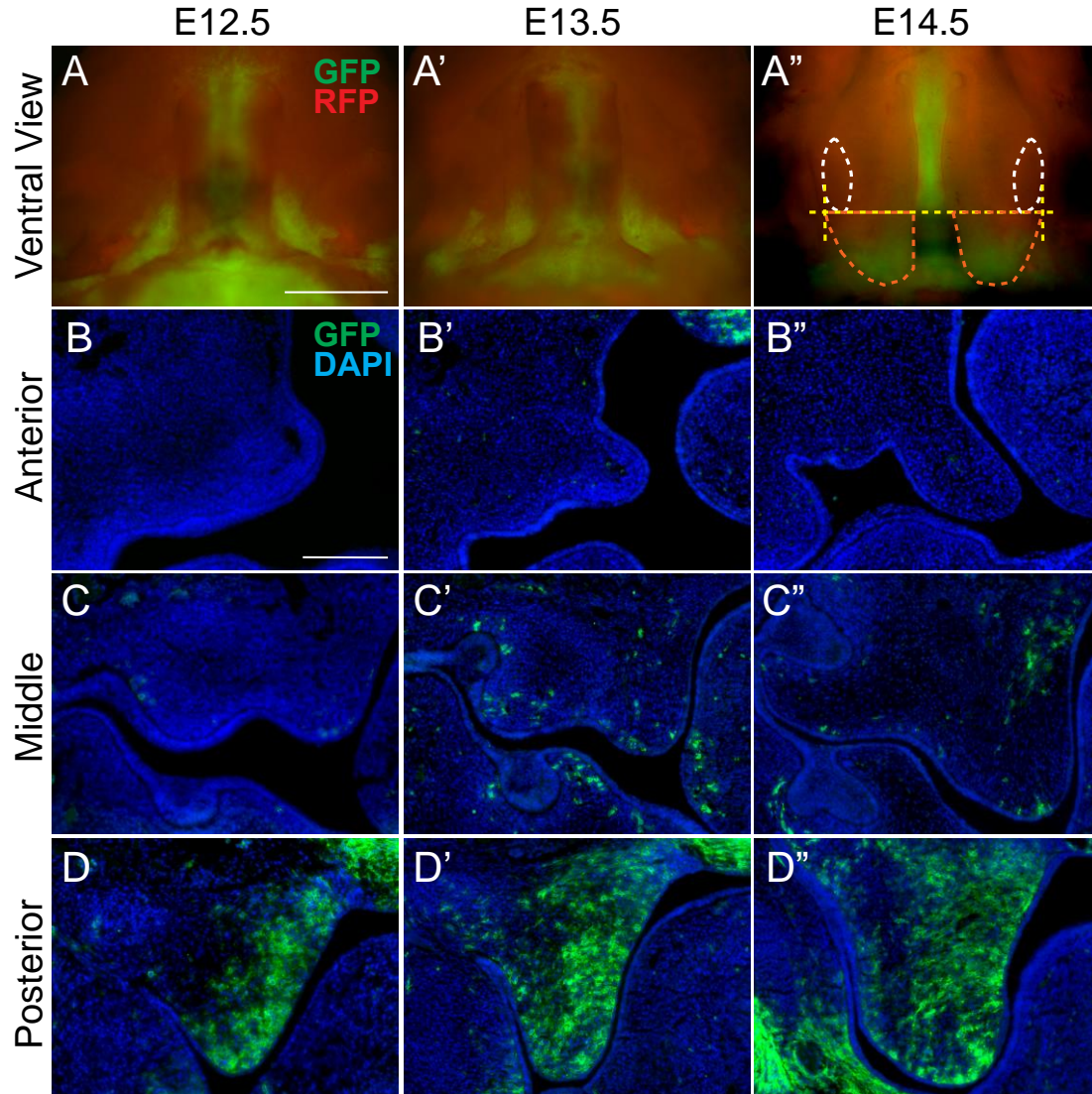


Supplemental Figure 2. Deletion of *Yap/Taz* with *K14*^{Cre} does not disrupt secondary palatogenesis. (A-B'') Images of H&E staining show palatal shelves of E16.5

Yap^{fl/fl}; *Taz*^{fl/fl}; *K14*^{Cre} embryo fused normally with no remaining medial epithelial seam (A-A''), similar to *Yap*^{fl/fl}; *Taz*^{fl/fl} control (B-B''). Scale bar=1mm.



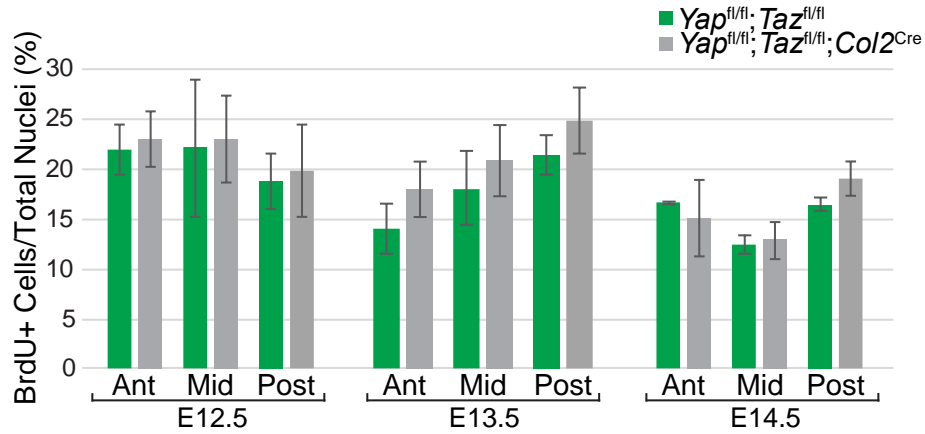
Supplemental Figure 3. Deletion of *Yap/Taz* with *Osr2^{Cre}* results in embryonic lethality and large blood-filled lesions. (A-D') Images of H&E stained coronal sections show blood-filled lesions in the mandible of *Yap^{fl/fl}; Taz^{fl/fl}; Osr2^{Cre}* mutant embryos at E13.5 (B, B') and E14.5 (D, D') that were not present in the *Yap^{fl/fl}; Taz^{fl/fl}* control embryos (A, A', C, C'). Scale bar=200 μ m. (E-F') Immunofluorescence with antibody against E-cad (green) and DAPI staining (blue) show that the mandibular lesion in the *Yap^{fl/fl}; Taz^{fl/fl}; Osr2^{Cre}* embryo appears to be a tissue space created by the separation of the E-cad labelled epithelium (green) from the underlying mesenchyme. Scale bar=100 μ m.



Supplemental Figure 4. *Col2*^{Cre} drives recombination in a subset of mesenchymal cells in the posterior palatal shelf. (A-A'') Images of ventral views of the palatal shelves in *R26R^{mTmG}; Col2^{Cre}* embryos at E12.5 (A), E13.5 (A'), and E14.5 (A'') show that in the palatal shelves, GFP (green) was specifically expressed in the posterior palatal shelf, indicating *Col2*^{Cre} recombination was specific to this region. Note, outside of the palatal shelves, there was also GFP expression in the nasal and cranial base cartilages. The molar placodes are circled by the white dashed lines and excision cuts are represented by yellow dashed lines to show the posterior palatal shelf tissue (outlined by orange dashed lines) collected for the RNA-Seq experiment in A''. Scale bar=1mm. (B-D'') Coronal sections stained with antibody against GFP

showing GFP expression in a subset of mesenchyme cells in the posterior palatal shelves at E12.5 (D), E13.5 (D'), and E14.5 (D"). There were a few scattered GFP+ cells in the middle palatal shelf region at E13.5 (C') and E14.5 (C") and no GFP expression observed in the anterior palate (B-B"). Scale bar=200 μ m.

Supplemental Figure 5.

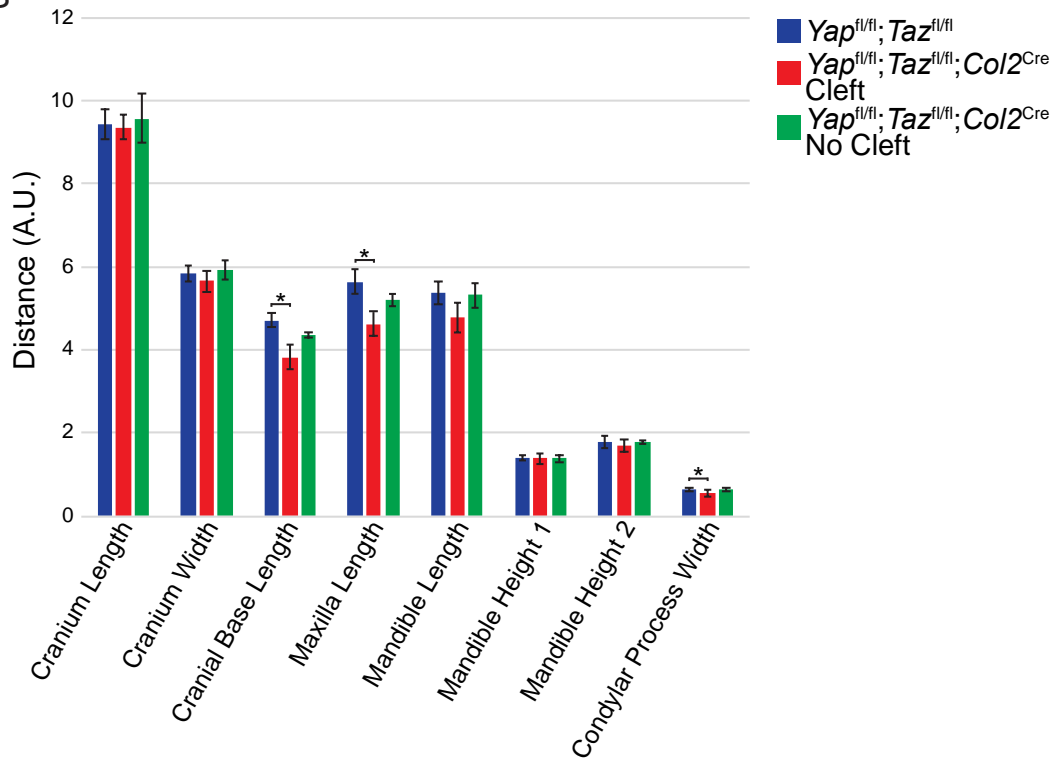


Supplemental Figure 5. Deletion of *Yap/Taz* with *Col2^{Cre}* does not affect proliferation in the palatal shelf mesenchyme. Graph of percentage of BrdU+ cells relative to total nuclei in the palatal shelf mesenchyme in the anterior (Ant), middle (Mid), and posterior (Post) of the palatal shelves in *Yap^{fl/fl}; Taz^{fl/fl}* control and *Yap^{fl/fl}; Taz^{fl/fl}; Col2^{Cre}* embryos at E12.5 (N=7), E13.5 (N=5), and E14.5 (N=4). There was no significant difference in proliferation between control and mutant embryos in any region of the secondary palate mesenchyme at any timepoint.

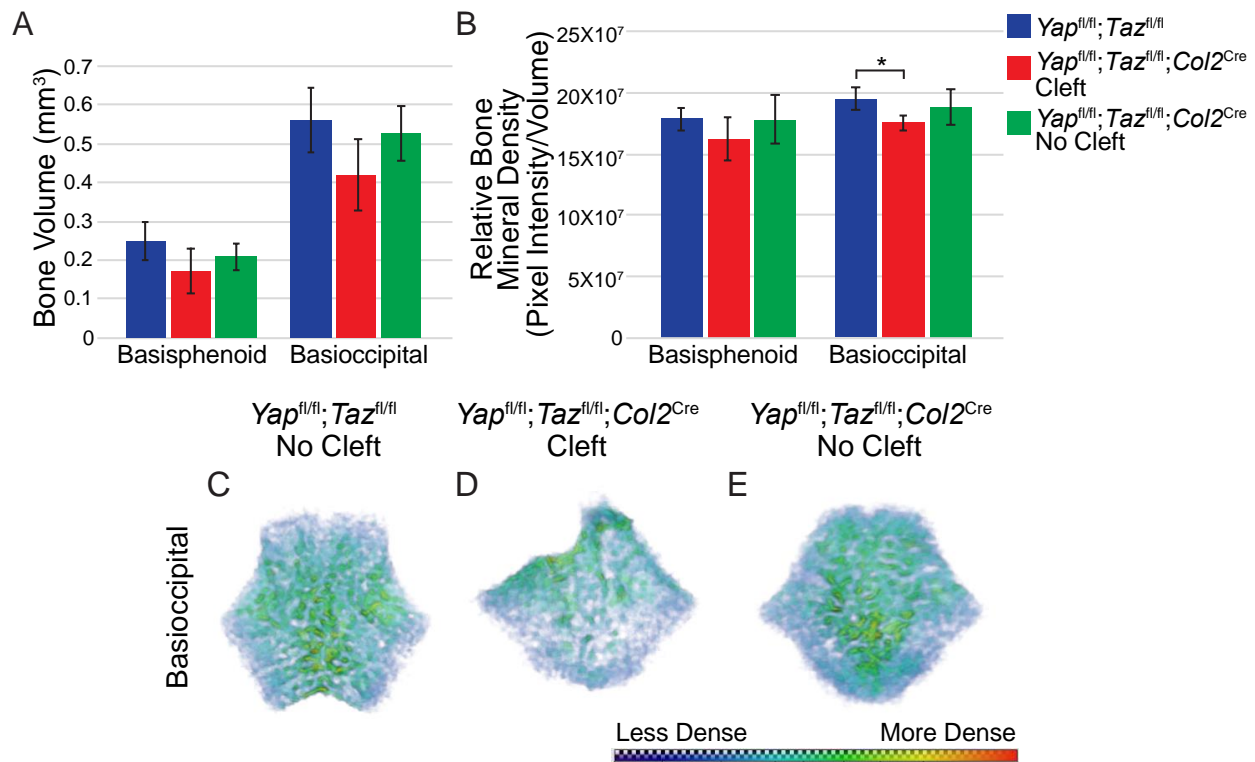
A

Measurement	Description
Cranium Length	Most posterior point of the occipital bone to the most anterior point of the nasal bone
Cranium Width	Distance between most lateral points on the squamosal bones
Cranial Base Length	Most posterior point of the basioccipital bone to most anterior point of the sphenoid
Maxilla Length	Most anterior point of the incisor alveolus to most posterior point of the basisphenoid
Mandible Length	Most superior-posterior point of the condyle to the most inferior-anterior point of the incisor alveolus
Mandible Height 1	Most anterior point of the molar alveolus to most inferior point of the lower border of the mandible
Mandible Height 2	Apex of the coronoid process to the most inferior point of the lower border of the mandible
Condylar Process Width	Distance between the most anterior and posterior points of the condylar process

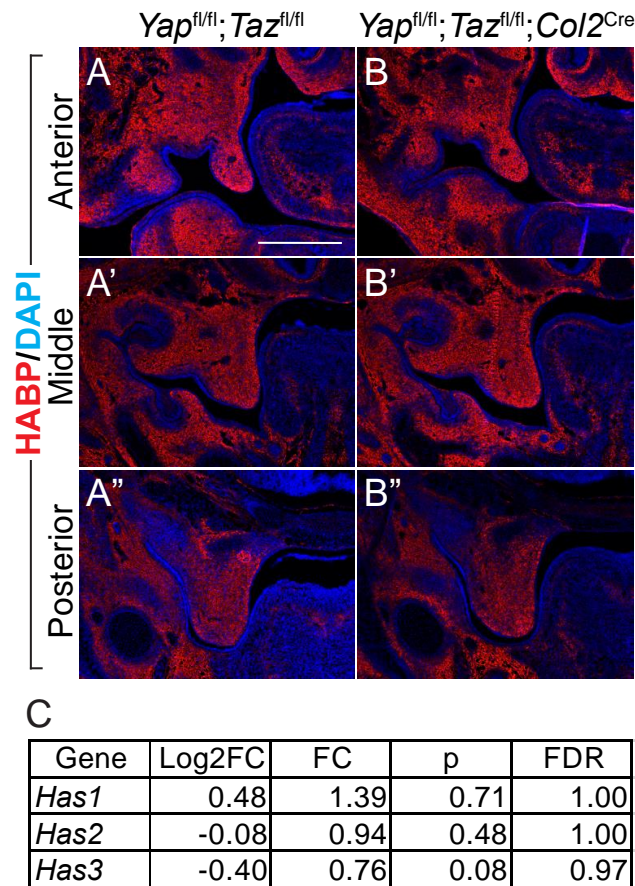
B



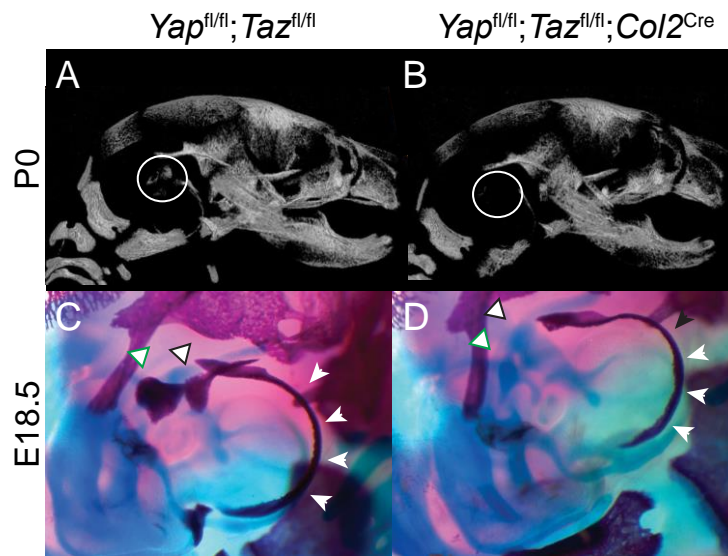
Supplemental Figure 6. Deletion of *Yap/Taz* with *Col2^{Cre}* results in a decrease in cranial base and maxilla length compared to control. (A) Table describing measurements taken on μ CT of *Yap^{fl/fl}; Taz^{fl/fl}* control (N=4) and *Yap^{fl/fl}; Taz^{fl/fl}; Col2^{Cre}* embryos with clefts (N=3) and without clefts (N=2) at E18.5. (B) Graph shows a significant decrease in the cranial base length, maxilla length, and condylar process width in *Yap^{fl/fl}; Taz^{fl/fl}; Col2^{Cre}* embryos with clefts compared to control. * $p < 0.05$.



Supplemental Figure 7. Deletion of *Yap/Taz* with *Col2^{Cre}* results in a decrease in bone mineral density but not volume in some skull bones that undergo endochondral ossification compared to control. (A-B) Graphs of the bone volume (A) and relative bone mineral density (B) of *Yap^{fl/fl}; Taz^{fl/fl}* control (N=4) and *Yap^{fl/fl}; Taz^{fl/fl}; Col2^{Cre}* embryos with clefts (N=3) and without clefts (N=2) at E18.5. There was no difference in bone volume of the basisphenoid or basioccipital (A); however, the basioccipital had a significant decrease in bone density in the *Yap^{fl/fl}; Taz^{fl/fl}; Col2^{Cre}* embryos with clefts compared to control. (C-E) Renderings of the basioccipital bone with the color representing the bone density (scale showing blue is less dense and red is more dense bone). Note the mineral area and density was less in the *Yap^{fl/fl}; Taz^{fl/fl}; Col2^{Cre}* embryos with clefts relative to the control or *Yap^{fl/fl}; Taz^{fl/fl}; Col2^{Cre}* embryos without clefts. * $p < 0.05$.



Supplemental Figure 8. Hyaluronic acid expression in the palatal shelf mesenchyme is not affected by deletion of *Yap/Taz*. (A-B”) Immunofluorescence with hyaluronic acid binding protein (HABP, red) and DAPI (blue) staining shows that the levels of hyaluronic acid were similar in *Yap^{fl/fl};Taz^{fl/fl};Col2^{Cre}* mutant (B-B”) and *Yap^{fl/fl};Taz^{fl/fl}* control (A-A”) embryos throughout the palatal shelves at E14.5. Scale bar=200μm. (C) Table of RNA-Seq data shows there was no significant difference in transcriptional levels of *Has1*, *Has2*, and *Has3* in *Yap^{fl/fl};Taz^{fl/fl};Col2^{Cre}* samples compared to control. FC=fold change, FDR=false discovery rate.



Supplemental Figure 9. Deletion of *Yap/Taz* with *Col2*^{Cre} results in decreased mineralization of the ear ossicles. (A,B) Lateral views of μ CT renderings of P0 skulls show that while the ear ossicles were mineralized and visible in the control (A, white circle), the bones of the ear were not ossified in the *Yap*^{fl/fl};*Taz*^{fl/fl};*Col2*^{Cre} embryo at this stage (B, white circle). (C,D) Skeletal preps of E18.5 skulls show that the tympanic ring was mineralized in both the *Yap*^{fl/fl};*Taz*^{fl/fl} control and *Yap*^{fl/fl};*Taz*^{fl/fl};*Col2*^{Cre} mutant (white arrowheads), however, while the malleus (black outlined arrow) and incus (green outlined arrow) were mineralizing in the control at this stage (C), there was no mineralization of these bones in the mutant, and only the cartilage templates were visible (D).

Supplemental Table 1.

Mouse	Genetics	MGI	Reference
<i>R26R</i> ^{mT/mT}	Gt(ROSA)26Sor ^{tm4(ACTB-tdTomato,-EGFP)Luo}	3716464	Muzumdar et al., 2007
<i>Yap</i> ^{fl/fl}	<i>Yap1</i> ^{tm1.1Eno}	5446483	Xin et al., 2011
<i>Taz</i> ^{fl/fl}	<i>Wwtr1</i> ^{tm1.1Eno}	5544289	Xin et al., 2011
<i>K14</i> ^{Cre}	Tg(KRT14-cre)1Amc	2445832	Dassule et al., 2000
<i>Col2</i> ^{Cre}	Tg(Col2a1-cre)1Bhr	2176070	Ovchinnikov et al., 2000
<i>Osr2</i> ^{Cre}	<i>Osr2</i> ^{tm2(cre)Jian}	3768549	Lan et al., 2007

Supplemental Table 1. Mouse lines utilized in experiments.

Supplemental Table 2.

Palatal Shelf Media Component	Source	Catalog Number
F12 Ham's Nutrient Mix Media	UCSF Cell Culture Facility	AB002-181C01
Streptomycin/Penicillin (50U/ml)	Gibco	10378016
Ascorbic Acid (0.2 mg/ml)	Sigma-Aldrich	95209
Bovine Serum Albumin (0.1%)	Sigma-Aldrich	A1595

Supplemental Table 2. Media used for palatal shelf cultures.

Supplemental Table 3.

Gene	Log2FC	FC	p	FDR
<i>Ibsp</i>	2.690	6.451	3.87E-07	0.003
<i>Phex</i>	1.894	3.718	1.07E-05	0.020
<i>Loxl4</i>	1.773	3.418	5.91E-07	0.003
<i>Cgref1</i>	1.703	3.256	1.05E-05	0.020
<i>Phospho1</i>	1.647	3.132	3.12E-07	0.003
<i>Lsamp</i>	1.596	3.024	1.82E-20	3.71E-16

Supplemental Table 3. Transcriptional levels of most differentially expressed genes in the posterior palatal shelves between *Yap^{fl/fl};Taz^{fl/fl};Col2^{Cre}* mutant and *Yap^{fl/fl};Taz^{fl/fl}* control. Most differentially expressed genes in the posterior palate of *Yap^{fl/fl};Taz^{fl/fl}* control and *Yap^{fl/fl};Taz^{fl/fl};Col2^{Cre}* mutant with false discovery rate (FDR) less than 0.05, log2FC greater than 1.5 and less than -1.0, and raw counts greater than 100. All genes listed were expressed at decreased levels in mutant compared to control.

Supplemental References:

Dassule HR, Lewis P, Bei M, Maas R, McMahon AP. 2000. Sonic hedgehog regulates growth and morphogenesis of the tooth. *Development*. 127(22):4775–4785.

Lan Y, Wang Q, Ovitt CE, Jiang R. 2007. A unique mouse strain expressing Cre recombinase for tissue-specific analysis of gene function in palate and kidney development. *Genesis*. 45(10):618–624.

Muzumdar MD, Tasic B, Miyamichi K, Li L, Luo L. 2007. A global double-fluorescent Cre reporter mouse. *Genesis*. 45(9):593–605.

Ovchinnikov DA, Deng JM, Ogunrinu G, Behringer RR. 2000. Col2a1-directed expression of Cre recombinase in differentiating chondrocytes in transgenic mice. *Genesis*. 26(2):145–146.

Xin M, Kim Y, Sutherland LB, Qi X, McAnally J, Schwartz RJ, Richardson JA, Bassel-Duby R, Olson EN. 2011. Regulation of insulin-like growth factor signaling by Yap governs cardiomyocyte proliferation and embryonic heart size. *Sci Signal*. 4(196):ra70.